

000
001
002
003
004
005
006
007
008
009
010
011
012
013
014
015
016
017
018
019
020
021
022
023
024
025
026
027
028
029
030
031
032
033
034
035
036
037
038
039
040
041
042
043
044
045
046
047
048
049
050
051
052
053

Using GPLVM for Inverse Kinematics on Non-cyclic Data

Anonymous Author(s)

Affiliation

Address

email

Abstract

We apply the Gaussian Process Latent Variable Model (GPLVM) to tackle the inverse kinematic problem in character animation during a ball catching scenario. The goal is to generate realistic upper-body movements with only the tip of the hand specified as the constraint. We ran a series of motion capture experiments to capture the body movement in a subject as he performs a ball catching task and then learn a scaled GPLVM. The ball catching scenario allows us to test the use of GPLVM to represent non-cyclic set of movements with plenty of style variation.

1 Introduction

Inverse kinematics (IK) is a very common task encountered in the field of computer animation and robotics. Its goal is to generate a solution for the degree-of-freedom (e.g. joint angles) given a small set of constraints, such as the location of the end effector. This is almost always an under-determined problem; although it is trivial to find a solution, finding a good solution is an ongoing research topic [1, 2, 3, 4]. Specifically in character animation, we want to obtain poses that appear natural. In this paper, we present an inverse-kinematic solution based on the Gaussian Process Latent Variable Model (GPLVM) for ball catching.

To obtain natural poses in an IK, one could learn from examples of real characters. Examples of example-based IK include [5, 6, 7, 8, 1]. Due to its flexibility and good performance, we have set out to use the method by [1] to solve the IK task for a ball catching scenario. The method uses a scaled GPLVM to represent the likelihood of the poses. However, their work has been mostly tested on cyclic data set such as walking or sequences with small style variations. On the other hand, the ball catching movement involves many different styles of movement.

2 Gaussian Process Latent Variable Model

2.1 Probabilistic PCA

Probabilistic PCA (PPCA) is a latent variable model which maps the latent space variables, $\mathbf{X} = [\mathbf{x}_1 \mathbf{x}_2 \dots]$ into the observation variables, $\mathbf{Y} = [\mathbf{y}_1 \mathbf{y}_2 \dots]$ through

$$\mathbf{y}_n = \mathbf{W}\mathbf{x}_n + \eta.$$

$\mathbf{W} \in \mathcal{R}^{D \times q}$ denotes the mapping coefficient where D and q are the dimensions of the observation and latent space variables respectively. η represents the zero-mean Gaussian distributed noise term with unit covariance:

$$p(\eta_n | \beta) = N(\eta_n | \mathbf{0}, \beta^{-1} \mathbf{I}),$$

where β is the inverse variance. Assuming independence across data points, the conditional probability of the data is given by

$$p(\mathbf{Y}|\mathbf{X}, \mathbf{W}, \beta) = \prod_{n=1}^N N(\mathbf{y}_n | \mathbf{W}\mathbf{x}_n \beta^{-1} \mathbf{I}).$$

If we pick the prior for the latent variables \mathbf{X} to be a zero-mean Gaussian with unit covariance, we can marginalize the latent variables \mathbf{X} to get

$$p(\mathbf{Y}|\mathbf{W}, \beta) = \frac{1}{(2\pi)^{\frac{DN}{2}} |\mathbf{C}|^{\frac{D}{2}}} \exp\left(-\frac{1}{2} \text{tr}(\mathbf{C}^{-1} \mathbf{Y}\mathbf{Y}^T)\right),$$

where the covariance is $\mathbf{C} = \mathbf{W}\mathbf{W}^T + \beta^{-1} \mathbf{I}$.

2.2 GPLVM as the dual of PPCA

If we marginalize over the mapping \mathbf{W} instead of the latent variables \mathbf{X} , and assuming a Gaussian prior of the mapping, we get

$$p(\mathbf{Y}|\mathbf{X}, \beta) = \frac{1}{(2\pi)^{\frac{DN}{2}} |\mathbf{K}|^{\frac{D}{2}}} \exp\left(-\frac{1}{2} \text{tr}(\mathbf{K}^{-1} \mathbf{Y}\mathbf{Y}^T)\right),$$

where $\mathbf{K} = \mathbf{X}\mathbf{X}^T + \beta^{-1} \mathbf{I}$. Note the duality between the above two equations. We can interpret the above likelihood as a product of D independent Gaussian processes by rewriting it as

$$p(\mathbf{Y}|\mathbf{X}, \beta) = \prod_{i=1}^D \frac{1}{(2\pi)^{\frac{N}{2}} |\mathbf{K}|^{\frac{D}{2}}} \exp\left(-\frac{1}{2} \mathbf{y}_{:,i}^T \mathbf{K}^{-1} \mathbf{y}_{:,i}\right),$$

where $\mathbf{y}_{:,i}$ is the i th column of \mathbf{Y} . Here, the Gaussian process creates a map from the latent space to the data space. We can learn the mapping through maximum likelihood with respect to \mathbf{X} . This is referred to as the Gaussian Process Latent Variable Model (GPLVM). We now extend this by allowing for non-linear processes by defining a non-linear kernel such as the RBF kernel

$$k(\mathbf{x}, \mathbf{x}') = \alpha \exp\left(-\frac{\gamma}{2} \|\mathbf{x} - \mathbf{x}'\|\right) + \delta_{\mathbf{x}, \mathbf{x}'} \beta^{-1},$$

here $\delta_{\mathbf{x}, \mathbf{x}'}$ denotes the Kronecker delta and α, β, δ are parameters to the kernel. We can form \mathbf{K} with $\mathbf{K}_{i,j} = k(\mathbf{x}_i, \mathbf{x}_j)$. Note that when we jointly optimise the likelihood for the latent space variables \mathbf{X} and the parameters α, β, γ , the cost function will contain many local minima as it is not unique even in the linear case.

3 Inverse Kinematics with GPLVM

Following [1], we can leverage the dimensionality reduction provided by GPLVM to project the character data into a low-dimensional latent space while learning the probability distribution function of the poses in the latent space. This distribution can then be used to select a good pose for the IK problem.

3.1 Character Model

The character pose is determined by a feature vector containing joint angles and the kinematic chain root position. We parameterize the joint angles using quaternions to avoid singularity at the cost of adding an extra dimension (per joint) to the representation [9]. The trade-off is made as such since it is difficult to avoid singularities just by performing a space rotation [1] for an unpredictable and varied arm movement as encountered during the catching task.

3.2 Model Learning

We apply a slight modification to the GPLVM model presented earlier by adding a scaling term to each of the observed variable \mathbf{y} [1]. This can be modeled by using different kernel function

108 $k(\mathbf{x}, \mathbf{x}')/s_k^2$ for each observation dimension. Alternatively, one could use different covariance func-
 109 tion \mathbf{K} for each dimension [10]. This takes into account the different variance in each of its dimen-
 110 sion - necessitated by the different characteristic.

111 To learn the GPLVM representation of the training data $\{\mathbf{y}_i\}$, we use the following priors for the
 112 unknown latent variable and parameters: $p(\mathbf{x}) = N(0, \mathbf{I})$ and $p(\alpha, \beta, \gamma) = \alpha^{-1}\beta^{-1}\gamma^{-1}$. We can
 113 then maximize the posterior
 114

$$115 \quad p(\{\mathbf{x}_i\}, \alpha, \beta, \gamma, \{s_k\} | \{\mathbf{y}_i\}) = p(\{\mathbf{y}_i\} | \{\mathbf{x}_i\}, \alpha, \beta, \gamma, \{s_k\}) \left(\prod_i p(\mathbf{x}_i) \right) p(\alpha, \beta, \gamma)$$

116 by minimizing the objective function corresponding to the negative log posterior
 117

$$118 \quad L_{GP} = \frac{D}{2} \ln |\mathbf{K}| + \frac{1}{2} \sum_k s_k^2 \mathbf{Y}_k^T \mathbf{K}^{-1} \mathbf{Y}_k + \frac{1}{2} \sum_i \|\mathbf{x}_i\|^2 + \ln \frac{\alpha\beta\gamma}{\prod_k s_k^N}$$

119 with respect to the unknowns.
 120
 121

122 3.3 Pose Synthesis

123 Once the scaled GPLVM has been learned from training data, we can use this model to calculate
 124 the posterior probability of a new pose as per Gaussian process regression. We can maximize this
 125 posterior by minimizing the objective function

$$126 \quad L_{IK}(\mathbf{x}, \mathbf{y}) = \frac{\|\mathbf{S}(\mathbf{y} - \mathbf{f}(\mathbf{x}))\|^2}{2\sigma^2(\mathbf{x})} + \frac{1}{2} \ln \sigma^2(\mathbf{x}) + \frac{1}{2} \|\mathbf{x}\|^2$$

127 where

$$128 \quad \mathbf{f}(\mathbf{x}) = \mu + \bar{\mathbf{Y}}^T \mathbf{K}^{-1} \mathbf{k}(\mathbf{x})$$

$$129 \quad \sigma^2(\mathbf{x}) = k(\mathbf{x}, \mathbf{x}) - k(\mathbf{x})^T \mathbf{K}^{-1} k(\mathbf{x}).$$

130 Here, $\bar{\mathbf{Y}}$ is the mean (μ) subtracted matrix of observed variables and $k(\mathbf{x})_i = k(\mathbf{x}, \mathbf{x}_i)$.
 131

132 The inverse kinematics problem of solving for a pose given some constraints can be solved by
 133 optimizing L_{IK} with respect to \mathbf{x} and \mathbf{y} with some constraint $C(\mathbf{y}) = 0$. More formally, we want
 134 to solve for:

$$135 \quad \arg \max_{\mathbf{x}, \mathbf{y}} L_{IK}(\mathbf{x}, \mathbf{y})$$

$$136 \quad \text{s.t. } C(\mathbf{y}) = 0.$$

137 4 Experiments and Results

138 4.1 Motion Capture Experiment

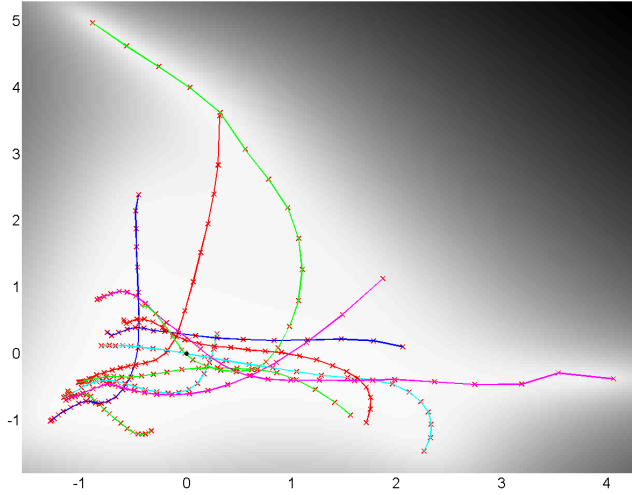
139 We motion captured a sitted subject upper body movement (excluding the left arm) using a set of 21
 140 markers and instructed the subject to catch the ball thrown towards him with his right hand. Each
 141 trial starts with the subject taking a pre-defined ‘home’ pose. We process the motion capture data
 142 into a feature vector \mathbf{y} containing the upper torso, head, and arm joint angles as well as the position
 143 of the upper torso. The data is downsampled from 100 Hz to 25 Hz.
 144

145 4.2 Learning the scaled GPLVM

146 We use the Scaled Conjugate Gradient method [11] to optimize the L_{GP} for learning the scaled
 147 GPLVM representation. In our experiment, the dataset was not sufficiently large enough to war-
 148 rant the use of fast approximations through the information vector machine [1, 12] or other sparse
 149 Gaussian Process representations [13, 14].
 150

151 Using a 2 dimensional latent space, we obtain the latent space representation shown in Figure 1.
 152 The intensity of the background indicates the uncertainty of the mapping. A lighter pixel indicates
 153
 154

162 lower uncertainty (higher precision). The different colored traces represents the different latent space
163 trajectory of each catch trial. Due to the non-cyclic nature of the character pose sequence, we do not
164 get a cyclic trajectory in the latent space as often seen in various latent space modeling of human
165 movement examples [1, 15, 10]. We can see that all the trajectories originate from the bottom-left
166 corner of the latent space; this corresponds to the ‘home’ pose at the start of the experiment.
167



169
170
171
172
173
174
175
176
177
178
179
180
181
182
183
184
185
186
187
188
189
190
191
192
193
194
195
196
197
198
199
200
201
202
203
204
205
206
207
208
209
210
211
212
213
214
215

Figure 1: Learned latent space for 11 ball catching sequences. Lines indicate latent space trajectory of each sequence. Red crosses are the actual training points.

4.3 Solving for the Inverse Kinematics

We proceed to use the learned model to perform inverse kinematics as described in subsection 3.3. In the experiment, we set constraints on the position of the tip of the hand. We use the Sequential Quadratic Programming method as implemented in Matlab’s `fmincon` function to solve the non-linear constrained optimization problem. Note that both the constraints and the objective function are nonlinear. The nonlinearity of the constraints comes from the rigid transformations needed to transform the observation variable y into the hand position. We initialize the optimizer by picking a point in the vicinity of the ‘home’ pose of the latent space and at every iteration, the initialization is updated to use the result of the previous optimization step. This has the benefit of giving some amount of temporal coherence which is important to achieve smooth character motion.

We first ran the inverse kinematic solver on one of the training data set. The result is shown in Figure 2. We can see that the inverse kinematic solution manages to generate poses which gives hand position close to the specified (constraint) trajectory.

A different set of IK tests are performed whereby the constraint trajectories do not come from the training set. An example of the result is shown in Figure 3. Here, the generated poses fail to meet the constraints specified. Furthermore, the latent space trajectory (not shown) snakes haphazardly through the latent space.

5 Discussion

The inability of the method to solve the IK problem in a ball catching scenario comes as a surprise to us in light of the success by [1] in using this method to solve the IK problem. We thus suspect that scaled GPLVM is not suitable for modeling non-cyclic and diverse movements.

We have tried using higher dimensional latent space model to improve the result to no avail. As mentioned before, the objective function is non-convex and thus the optimization process might be stuck in local minima. We have tried adding the model smoothing process used in [1] which involves

216
217
218
219
220
221
222
223
224
225
226
227
228
229
230
231
232
233
234
235
236
237
238
239
240
241
242
243
244
245
246
247
248
249
250
251
252
253
254
255
256
257
258
259
260
261
262
263
264
265
266
267
268
269

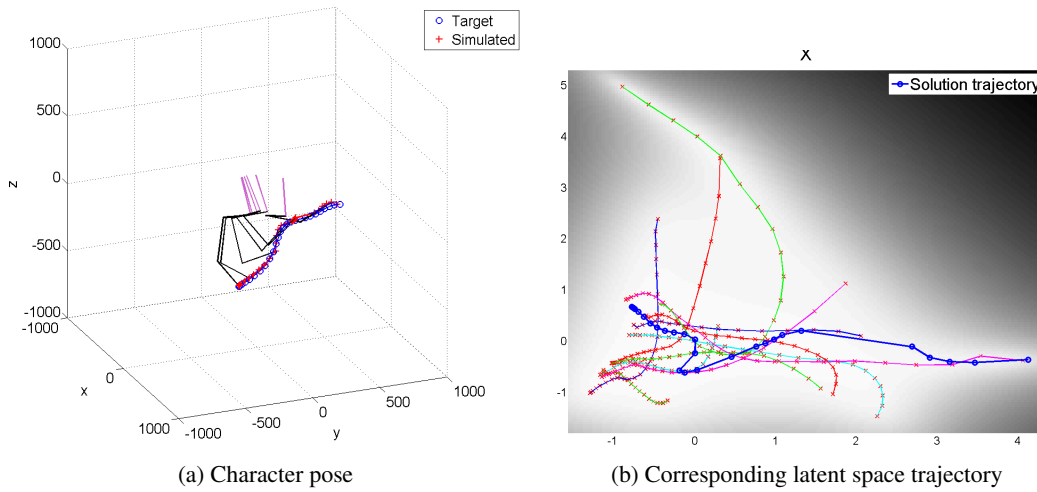


Figure 2: Inverse kinematic result on a trajectory in the training set

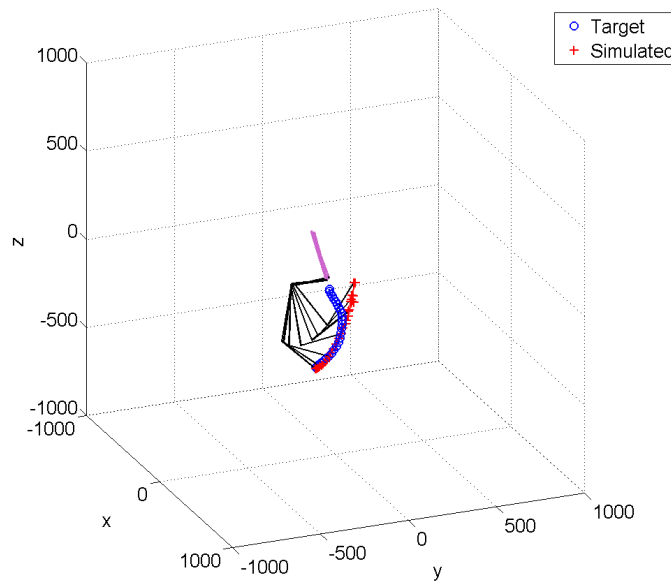


Figure 3: Inverse kinematic result on a trajectory in the test set.

creating smoother version of the model to be used as a starting model to search in the optimization process. This however, does not seem to improve the result obtained.

We suspect that the main reason for the failure of GPLVM to generate a usable latent space stems from the lack of a smooth mapping from the observed space to the latent space even though the converse is true. This causes points close together in data space to not necessarily be close in latent space. We can clearly see this behavior in Figure 1 – the ‘home’ locations for the different sequences in the latent space can be fairly far apart even though they are very similar in the data (character pose) space. This is a commonly observed problem in GPLVM and often causes jumps in the latent space trajectory [10, 15, 16]. In [1], velocity variables are augmented to the observation variable possibly with the intent of alleviating this problem. However when we tried this, we found no significant change to the latent space.

There are several modifications proposed to the GPLVM that can enforce this smoothness. One such proposal is the use of back constraints [17]. Back constraints constraint the latent space to be a

smooth function of the observation space. Alternatively, one could incorporate a non-linear dynamic model in the latent space using the Gaussian Process Dynamical Models (GPDM) [16, 15]. Both the back constraint and GPDM has been shown to improve the quality of the learned latent space representation. Further extensions to the GPLVM that can possibly improve the result includes adding topological constraints to improve handling of motion style variations [18].

References

- [1] Keith Grochow, Steven L. Martin, Aaron Hertzmann, and Zoran Popović. Style-based inverse kinematics. In *ACM SIGGRAPH 2004 Papers*, SIGGRAPH '04, pages 522–531, New York, NY, USA, 2004. ACM.
- [2] Sethu Vijayakumar and Stefan Schaal. Learning inverse kinematics. In *Proceedings of International Conference on Intelligent Robots and Systems (IROS)*, pages 298–303, 2001.
- [3] Ferdinando Mussa-Ivaldi Massachusetts, Ferdinando A. Mussa-ivaldi, and Neville Hogan. Integrable solutions of kinematic redundancy via impedance control. *The International journal of robotics research*, 10(5):481, 1991.
- [4] Richard M. Murray, Zexiang Li, and S. Shankar Sastry. *A Mathematical Introduction to Robotic Manipulation*. Boca Raton : CRC Press, 1994.
- [5] George ElKoura and Karan Singh. Handrix: animating the human hand. In *Proceedings of the 2003 ACM SIGGRAPH/Eurographics symposium on Computer animation*, SCA '03, pages 110–119, Aire-la-Ville, Switzerland, Switzerland, 2003. Eurographics Association.
- [6] Lucas Kovar, Michael Gleicher, and Frédéric Pighin. Motion graphs. *ACM Transaction on Graphics*, 21:473–482, July 2002.
- [7] C. Rose, M.F. Cohen, and B. Bodenheimer. Verbs and adverbs: multidimensional motion interpolation. *Computer Graphics and Applications, IEEE*, 18(5):32–40, sep/oct 1998.
- [8] D.J. Wiley and J.K. Hahn. Interpolation synthesis of articulated figure motion. *Computer Graphics and Applications, IEEE*, 17(6):39–45, nov/dec 1997.
- [9] Andrew J. Hanson. Visualizing quaternions. In *ACM SIGGRAPH 2005 Courses*, SIGGRAPH '05, New York, NY, USA, 2005. ACM.
- [10] Neil D. Lawrence. The gaussian process latent variable model, 2006.
- [11] Martin Fodsllette and Miller. A scaled conjugate gradient algorithm for fast supervised learning. *Neural Networks*, 6(4):525–533, 1993.
- [12] Neil D. Lawrence, Matthias Seeger, and Ralf Herbrich. Fast sparse gaussian process methods: The informative vector machine. In *Advances in Neural Information Processing Systems 15*, pages 609–616. MIT Press, 2003.
- [13] Neil D. Lawrence. Learning for larger datasets with the gaussian process latent variable model. In *Proceedings of the 11th International Conference on Artificial Intelligence and Statistics*, 2007.
- [14] Joaquin Quiñero Candela and Carl Edward Rasmussen. A unifying view of sparse approximate gaussian process regression. *The Journal of Machine Learning Research*, 6:1939–1959, December 2005.
- [15] J.M. Wang, D.J. Fleet, and A. Hertzmann. Gaussian process dynamical models for human motion. *Pattern Analysis and Machine Intelligence, IEEE Transactions on*, 30(2):283–298, feb. 2008.
- [16] Jack M. Wang, David J. Fleet, and Aaron Hertzmann. Gaussian process dynamical models. In *NIPS*, pages 1441–1448. MIT Press, 2006.
- [17] Neil D. Lawrence and Joaquin Quiñero Candela. Local distance preservation in the gp-lvm through back constraints. In *Proceedings of the 23rd international conference on Machine learning*, ICML '06, pages 513–520, New York, NY, USA, 2006. ACM.
- [18] Raquel Urtasun, David J. Fleet, Andreas Geiger, Jovan Popović, Trevor J. Darrell, and Neil D. Lawrence. Topologically-constrained latent variable models. In *Proceedings of the 25th international conference on Machine learning*, ICML '08, pages 1080–1087, New York, NY, USA, 2008. ACM.